



# **A semi-implicit approach for sediment transport models with gravitational effects**

J. Garres-Díaz, E.D. Fernández-Nieto, G Narbona-Reina

## **► To cite this version:**

J. Garres-Díaz, E.D. Fernández-Nieto, G Narbona-Reina. A semi-implicit approach for sediment transport models with gravitational effects. Applied Mathematics and Computation, 2022, <10.1016/j.amc.2022.126938>. <hal-03247606>

**HAL Id: hal-03247606**

**<https://hal.science/hal-03247606v1>**

Submitted on 3 Jun 2021

**HAL** is a multi-disciplinary open access archive for the deposit and dissemination of scientific research documents, whether they are published or not. The documents may come from teaching and research institutions in France or abroad, or from public or private research centers.

L'archive ouverte pluridisciplinaire **HAL**, est destinée au dépôt et à la diffusion de documents scientifiques de niveau recherche, publiés ou non, émanant des établissements d'enseignement et de recherche français ou étrangers, des laboratoires publics ou privés.



HAL Authorization

# A semi-implicit approach for sediment transport models with gravitational effects

J. Garres-Díaz\*, E.D. Fernández-Nieto<sup>†</sup>, G. Narbona-Reina<sup>† ‡</sup>

April 28, 2021

## Abstract

In this work an efficient semi-implicit method, which is based on the theta method, for sediment bedload transport models with gravitational effects under subcritical regimes is proposed. Several families of models with gravitational effects are presented and rewritten under a general formulation that allows us to apply the semi-implicit method. In the numerical tests we focus on the application of a generalization of the Ashida-Michiue model, which includes the gradient of both the bedload and the fluid surface. Analytical steady states solutions (both lake at rest and non vanishing velocity) are deduced and approximated with the proposed scheme. In all the presented tests, the computational efforts are notably reduced thanks to the proposed method without losing the accuracy in the results.

**Keywords:** Sediment bedload transport, Shallow Water Exner model, gravitational effects, semi-implicit scheme.

---

\*Dpto. Matemáticas. Edificio Albert Einstein - Universidad de Córdoba, Spain, (jgarres@uco.es)

<sup>†</sup>Dpto. Matemática Aplicada I, Universidad de Sevilla, Spain (edofer@us.es,gnarbona@us.es)

<sup>‡</sup>All authors were partially supported by the Spanish project RTI2018-096064-B-C22 and FEDER

# 1 Introduction

The sediment transport phenomena is a problem of interest in the environmental field. Besides the typical application in the morphology of a river, the sphere of action of the sedimentation process is wide and it has a deep impact on its environment. Due to the flow of the river some particles are swept along the current. This material is taken mainly from the riversides and also from the bottom, being deposited downstream when the flow becomes weaker, either again on the riversides or in its mouth. This effect change the morphology of the river environment sometimes affecting to crops or to natural protected areas but also to fluvial navigation and coastal zones with the consequent impact in the economy and environmental aspects. It is also important the effect of the sediment transport process in the building of hydraulic structures like dams or bridges. Either the long-term erosion process or for example in torrential rain events or during the thaw, some of the sediment of the bottom can be dragged and may affect to the stability of these structures. Normally most of these important phenomena are long-term processes so there is a special interest on the development of efficient predictive techniques in order to prevent hazards or to better manage the surroundings.

Sediment transport occurs mainly through two phenomena: bedload and suspended load. Bedload entails the transport of sediment particles rolling or sliding on the bed and jumping into the flow and then resting on the bed again. Particles transported by suspension are supported by the surrounding fluid during a significant part of the current and may also be deposited. In this paper we focus on bedload sediment transport including gravitational effects that is an essential but not trivial task to take into account in the mathematical modeling.

When the bedload phenomena is under study, we must consider both, the hydrodynamical component and the morphodynamical one that are coupled. The Saint Venant Exner system is commonly used to describe the bedload sediment transport and it is a system composed on the well known Saint Venant (or Shallow Water) system for the hydrodynamics and a continuity equation to update the morphodynamical part. This continuity equation is called Exner equation [16], and it is defined in terms of the solid transport discharge that has to be prescribed. In the literature several models have been defined empirically to give this closure [30, 1, 17, 24, 37, 32]. Even if these models are largely used they provide some inconvenient properties for the system as the lack of a dissipative energy or the loss of the mass conservation, other important limitation being the validation range for just nearly horizontal sediment beds. An alternative to these empirical models has been presented in [18] where a complete Saint Venant Exner type model is derived from the Navier-Stokes equations, this model encompassing the former disadvantages.

In classical models, the solid transport discharge is defined in terms of the shear stress and the critical shear stress, or its normalized form called Shields parameter. Bedload models predict that there is no transport of sediment particles whenever the shear stress is smaller than the critical shear stress, see for instance [16, 30, 1, 17, 24, 37, 32].

The Shields parameter is defined as the ratio between the agitating and stabilizing forces on a deposited sediment particle. Lysne [29] showed experimentally for inclined sediment beds that the gravity is an important contributing action as agitating force, see also [20]. Nevertheless classical formulas consider that the shear stress is the unique agitating force. Therefore, gravitational forces play an essential role into the sediment transport, so they must be considered for the definition of an appropriate solid discharge for applications in general sloping beds.

Several forms to include gravitational effects in the solid transport discharge are found in the literature. The simplest one is to include a second order derivative in the Exner equation, which is neglected when the slope of the bed is smaller than the tangent of the repose angle of the material (see Tassi *et al.* [36]). Nevertheless, the form in which gravitational effects are usually included is

by modifying either the definition of the shear stress or the critical shear stress. Although these two kind of modifications might coincide in some particular cases for 1D horizontal domains, they are not equal in general.

Here we consider the inclusion of the gravitational effect in the solid transport discharge, which is defined in terms of the effective shear stress (see e.g. Fowler *et al.* [19]). This is discussed in detail by Fernández-Nieto *et al.* [18] showing that the solid discharge naturally incorporates gravitational effects, which are included in the effective shear stress. Let us also mention that the inclusion of gravitational effects in the effective shear stress is analogous for scalar or vector systems, that is, 1D or 2D horizontal domains. Nevertheless, when the modification of the critical shear stress is considered, the inclusion of gravitational effects for 2D domains is not an easy extension of the 1D case. See Kovacs and Parker [28], Seminara *et al.* [35] and Parker *et al.* [33] among others.

From the numerical point of view, bedload transport models have been usually discretized by means of explicit schemes in collocated and staggered meshes (see [6, 7, 31, 3, 25, 18] among many others). These problems are characterized by two different time scales: a small characteristic time for the hydrodynamical counterpart and a large characteristic time for the morphodynamical contribution. It makes the computational cost to be very high when explicit discretizations are used, even for simple models (e.g. Grass formula) without gravitational effects. In Bilanceri *et al.* [4] a comparison of explicit and implicit methods for bedload transport (without gravitational forces) is made, as function of the low/medium/high sediment-fluid interaction. They claim that the fully implicit scheme is too much expensive, and a linearization of the method based on the automatic differentiation software *Tapenade* [26] is made to solve the Grass model, showing that the computational cost is decreased, specially in the low interaction case.

Just a few works are devoted to numerical approximation of bedload models with gravitational effects. In these models, the difficulty from a numerical point of view is the presence of a non-linear elliptic counterpart in the Exner equation. As a consequence, its explicit discretization is computationally expensive. Tassi *et al.* [36] used a Discontinuous Galerkin method to approximate a Grass model with a diffusion term depending on the free surface gradient. Later, Morales de Luna *et al.* [31] used a duality method based on the Bermúdez-Moreno algorithm to solve the morphodynamical component of a Meyer-Peter & Müller model with gravitational effects, which is computationally more expensive.

Therefore, semi-implicit schemes are an interesting and promising alternative in the framework of bedload transport models. The method considered here is the one introduced by Casulli and co-worker for hydrostatic [11, 10, 8, 13] and non-hydrostatic [12, 14, 9] free surface flows in  $z$ -coordinates and isopycnal coordinates. In Bonaventura *et al.* [5] and Garres-Díaz and Bonaventura [23] this method was adapted to vertical multilayer discretization, showing its efficiency when it is applied to bedload transport with the simple Grass formula, and also for variable density flows.

Such a semi-implicit approach was used in Garegnani *et al.* [21, 22], where an analysis of the coupled and decoupled approach of the Exner equation is made, introducing also a semi-implicit method ([34]) for the system with movable bed, although they did not consider gravitational effects.

The main contribution of this work is a low-computational cost semi-implicit scheme for sediment transport problems solved through the Saint Venant Exner system introduced in [18] taking into consideration also gravitational effects, in long-time scale, i.e., slow processes. It is based on a reformulation of the solid transport discharge by rewriting the sign function. Furthermore, the proposed method could be easily adapted to a wide range of families of bedload models with gravitational effects, which is also described in this work. Thus, to our knowledge, this is the first efficient numerical scheme for general bedload models with gravitational effects.

Section 2 is devoted to present the model we use, as well as the reformulation of the solid transport discharge that we propose to apply the semi-implicit scheme to a wide family of models with grav-

itational effects. In Section 3 the semi-implicit method is detailed, and the numerical experiments are in Section 4. Finally, we present some conclusions in Section 5.

## 2 Saint Venant Exner system with gravitational effects

In this section we present the initial system for the hydrodynamical and morphodynamical counterparts. The solid transport discharge including gravitational effects is defined in Subsection 2.2. Once the chosen model is exposed, the reformulation of the solid transport discharge is proposed in Subsection 2.3, where we also analyze the steady solutions of the proposed model. Finally, we show in Subsection 2.4 how this reformulation could be easily adapted to a wide range of families of bedload models, depending on both the definition of the solid transport discharge and the effective shear stress.

### 2.1 Initial system

The base system is the well-known Saint Venant Exner system, which is obtained from the coupling of the Saint Venant system (hydrodynamical component) and the Exner equation (morphodynamical component). This model is deduced from the non-dimensional Navier-Stokes equations for the hydrodynamical part together with the Reynolds equation for the evolution of the granular layer, a detailed derivation and analysis of this model can be seen in Fernández-Nieto *et al.* [18]. Considering a 1D incompressible fluid with constant density  $\rho \in \mathbb{R}$ , the system reads

$$\begin{cases} \partial_t h + \partial_x q = 0, \\ \partial_t q + \partial_x (q^2/h) + gh\partial_x (h + b) = -\mathcal{F}, \\ \partial_t b + \partial_x Q_b = 0, \end{cases} \quad (1)$$

where  $(x, t)$  are the space and time variables,  $h(x, t)$  and  $u(x, t)$  the height and averaged horizontal velocity of the fluid, and  $q = hu$  is the discharge. The gravity acceleration is denoted by  $g$  and  $\mathcal{F}$  is a friction term between the fluid and the sediment layer  $b(x)$  which will be defined later. This sediment is transported according to the solid transport discharge  $Q_b$  that is defined by the chosen model for the bedload transport.

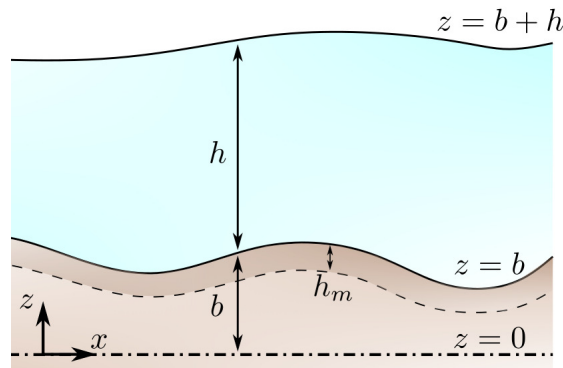


Figure 1: *Computational domain and notation.*

In the deduction presented in [18] the thickness of the sediment layer (denoted by  $b$  here and  $h_2$  in [18]) is subdivided in a lower static layer and a small upper movable layer whose height is

$h_m$  (see Figure 1). Simplified models are also presented there, which is the framework considered in this work. Assuming a quasi-uniform regime, the erosion rate equals the deposition rate and  $h_m$  can be estimated in terms of the the rest of unknowns of the problem.

Let us denote the shear stress by  $\tau$ , which can be written, in the framework of depth-averaged models, as  $\tau = \rho g h \mathcal{S}$  with  $\mathcal{S}$  a friction term, whose more common definitions are through the Manning ( $\mathcal{S} = n^2 u |u| h^{-4/3}$ ,  $n$  the Manning coefficient) or Darcy-Weisbach ( $\mathcal{S} = \xi u |u| / 8 g h$ ,  $\xi$  the Darcy-Weisbach coefficient) laws, depending on the averaged velocity  $u$ . Then, we can write

$$\frac{\tau}{\rho} = C |u| u, \quad \text{with} \quad \begin{aligned} C &= g n^2 h^{-1/3} & (\text{Manning law}), \\ C &= \xi / 8 & (\text{Darcy-Weisbach law}). \end{aligned} \quad (2)$$

An empirical formula is used to define the solid transport discharge as a closure to the system, for instance Grass [24], Meyer-Peter & Müller [30], Ashida & Michiue [1], among many others. For instance, when the classical Ashida & Michiue's model is chosen, it is written in nondimensional form as

$$\frac{Q_b}{Q} = \text{sgn}(\tau) \frac{17}{1 - \varphi} (\theta - \theta_c)_+ \left( \sqrt{\theta} - \sqrt{\theta_c} \right), \quad (3)$$

where  $\varphi$  is the porosity of the sediment bed,  $\text{sgn}(\cdot)$  is the sign function,  $(\cdot)_+$  the positive part, and  $Q = d_s \sqrt{g(1/r - 1)} d_s$  the characteristic discharge that is defined in terms of the gravity, the density ratio  $r = \rho_s / \rho$ , with  $\rho_s$  and  $d_s$  the density and the diameter of the sediment particles. Finally,  $\theta$  is the so-called Shields parameter, defined by

$$\theta = \frac{|\tau| d_s^2}{g (\rho_s - \rho) d_s^3},$$

with  $\theta_c$  the critical Shield stress.

A general formulation that includes a great number of classical models for the bedload solid transport discharge without gravitational effects may be written under the following compact form (see [18])

$$\frac{Q_b}{Q} = \text{sgn}(\tau) \frac{\alpha_1}{1 - \varphi} \theta^{\beta_1} (\theta - \alpha_2 \theta_c)_+^{\beta_2} \left( \sqrt{\theta} - \alpha_3 \sqrt{\theta_c} \right)^{\beta_3}, \quad (4)$$

with  $\alpha_i, \beta_i$   $i=1,2,3$  positive constants.

Some important drawbacks of these classical models for the bedload transport are: (i) they do not take into account gravitational effects, since they are derived using as hypothesis that the sediment free surface is almost constant  $\partial_x b \approx 0$ ; (ii) they do not satisfy a dissipative energy balance; (iii) the mass of sediment may be not conserved. In this work we study gravitational effects in models satisfying a dissipative energy balance. We consider the case of quasi-uniform regimes, where the movable thickness of sediment is set in terms of the velocity of the fluid. In these cases the mass conservation will not be guaranteed but it can be easily solved as detailed in the following subsection. Models including gravitational effects are presented in following subsections.

## 2.2 Solid transport discharge with gravitational effects

In this subsection, following [18], we present the generalization of the Ashida-Michiue and Meyer-Peter & Müller models under the assumption of a quasi-uniform regime. The general definition of the solid transport discharge is

$$Q_b = h_m v_b \sqrt{(1/r - 1) g d_s},$$

where  $h_m$  is the thickness of the movable bed and  $v_b$  the averaged sediment velocity. This velocity is defined in terms of the effective shear stress ( $\tau_{\text{eff}}$ ) as follows

$$v_b = \text{sgn}(\tau_{\text{eff}})(\sqrt{\theta_{\text{eff}}} - \sqrt{\theta_c})_+, \quad (5)$$

with

$$\theta_{\text{eff}} = \frac{|\tau_{\text{eff}}|/\rho}{(1/r - 1)gd_s},$$

where  $\tau_{\text{eff}}$  must be properly defined. Here, following [18], we consider (see discussion in Subsection 2.4)

$$\frac{\tau_{\text{eff}}}{\rho} = \frac{\tau}{\rho} - \frac{\vartheta gd_s}{r} \partial_x (rh + b), \quad \text{with} \quad \vartheta = \frac{\theta_c}{\tan \delta}, \quad (6)$$

being  $\delta$  the angle of repose of the material. Frequent values for these constants are  $\theta_c = 0.047$  and  $\vartheta = 0.1$ , that is  $\theta_c/\vartheta \approx \tan 25^\circ$  (see Fredsøe in [20]). Other possibilities are used in [15] and references therein.

We can establish the relation between  $\theta$  and  $\theta_{\text{eff}}$  by computing  $\tau$  from the previous equation, obtaining

$$\theta_{\text{eff}} = \left| \text{sgn}(u)\theta - \frac{\vartheta}{1-r} \partial_x (rh + b) \right|,$$

where  $\text{sgn}(u)$  is identified as the  $\text{sgn}(\tau)$  and we used the definition of  $\tau$  in (2).

In order to set the definition of  $h_m$  we will consider the case of a quasi-uniform regime, where  $h_m$  is defined by a closed formula as a function of the erosion and deposition rates (see [18] and references therein for further details). A possibility is to define

$$h_m = \frac{K_e d_s}{K_d (1 - \varphi)} (\theta_{\text{eff}} - \theta_c)_+, \quad (7)$$

with  $K_e, K_d$  constant parameters related to the erosion and deposition effects respectively. Let us remark that Fernández-Luque and Van Beek [17] observed in the experiments this linear relation between the thickness of the movable bed and the shear stress. Most of classical formulas consider this relation to obtain the solid transport discharge. This linear relation was also observed in Bagnold [2] by investigating the momentum transference because of the sediment particles and fixed bed interaction (see also [15]). Notice that the fact of using a closure formula for  $h_m$  as above may be the mass conservation fail, see [31]. Nevertheless, this problem is solved by defining  $h_m$  as the minimum between the definition (7) and the thickness of the erodible sediment layer. In this work we consider that this layer is large enough, since a fixed bedrock has not been taking into account.

By using the definition of  $h_m$  (7) we obtain the following formula of the solid transport discharge

$$\frac{Q_b}{Q} = \text{sgn}(\tau_{\text{eff}}) \frac{K_e}{K_d (1 - \varphi)} (\theta_{\text{eff}} - \theta_c)_+ (\sqrt{\theta_{\text{eff}}} - \sqrt{\theta_c})_+ \quad \text{where} \quad Q = d_s \sqrt{(1/r - 1)gd_s}. \quad (8)$$

Note that this is a generalized Ashida & Michiue's model (3), where the ratio between erosion and deposition effects is set to  $K_e/K_d = 17$ .

Another possibility is to define  $h_m$  as follows (see [35])

$$h_m = \frac{K d_s}{1 - \varphi} \sqrt{(\theta_{\text{eff}} - \theta_c)_+ (\sqrt{\theta_{\text{eff}}} + \sqrt{\theta_c})}. \quad (9)$$

In this case we obtain that the solid transport discharge is

$$\frac{Q_b}{Q} = \text{sgn}(\tau_{\text{eff}}) \frac{K}{(1-\varphi)} (\theta_{\text{eff}} - \theta_c)_+^{3/2}. \quad (10)$$

Note that in this case we obtain a generalized Meyer-Peter & Müller model, where the constant parameter is set to  $K = 8$ .

Finally, in [18] it is also deduced the following definition of the friction term between the fluid and the sediment layer, which is proportional to the difference of velocities

$$\mathcal{F} = \begin{cases} \frac{gh_m C}{r} \left( \partial_x(rh + b) + (1-r) \text{sgn}(\tau_{\text{eff}}) \tan \delta \right) & \text{if } \theta_{\text{eff}} > \theta_c, \\ \tau/\rho & \text{otherwise.} \end{cases} \quad (11)$$

**Remark 1.** Notice that this definition of  $\mathcal{F}$  coincides with the following definition of the friction between the fluid and the sediment layer:

$$\mathcal{F} = C|u - v|(u - v), \quad \text{where} \quad v = \begin{cases} u - \sqrt{gh_m/r} |\mathcal{P}|^{1/2} \text{sgn}(\mathcal{P}) & \text{if } \theta_{\text{eff}} > \theta_c, \\ 0 & \text{otherwise,} \end{cases}$$

being  $v$  the velocity of the sediment layer and  $\mathcal{P} = \partial_x(rh + b) + (1-r) \text{sgn}(\tau_{\text{eff}}) \tan \delta$ , for more details see [18].

In the next subsection the final model is reformulated in order to properly introduce a semi-implicit numerical scheme.

## 2.3 Reformulation of the bedload model with gravitational effects

Hereinafter we consider the model defined by (1), (8) and (11), corresponding to the generalization of the Ashida-Michiue Saint Venant Exner model including gravitational effects and a friction term proportional to the difference of velocities between the fluid and the sediment layer. Our goal in this work is to develop a semi-implicit scheme based on splitting the system as a stiff part (gravitational terms) with a high impact over the stability CFL condition and a non-stiff contribution. Looking for a more convenient writing of the system in that sense using (2), (6) and setting  $\text{sgn}(W) = W/|W|$ , the solid transport discharge (8) is reformulated as

$$Q_b = \frac{\tau_{\text{eff}}}{\rho} \tilde{q}_b = \tilde{q}_b (C|u|u - k_1 \partial_x(b + h) - k_2 \partial_x b) \quad (12a)$$

with

$$k_1 = \vartheta g d_s, \quad k_2 = \vartheta g d_s (1/r - 1) \quad (12b)$$

positive constants, and

$$\tilde{q}_b = \frac{\rho Q}{|\tau_{\text{eff}}|} \frac{K_e}{K_d(1-\varphi)} (\theta_{\text{eff}} - \theta_c)_+ \left( \sqrt{\theta_{\text{eff}}} - \sqrt{\theta_c} \right). \quad (12c)$$

For convenience to apply the numerical scheme, the final system is written in terms of the free surface level. Then, defining  $\eta = b + h$  and combining the first and third equations in (1), the final system reads

$$\begin{cases} \partial_t \eta + \partial_x (q + \tilde{q}_b C u |u| - \tilde{q}_b k_1 \partial_x \eta - \tilde{q}_b k_2 \partial_x b) = 0, \\ \partial_t q + \partial_x (q^2/h) + g(h + C h_m) \partial_x \eta = -g C h_m (1/r - 1) (\partial_x b + \text{sgn}(v_b) \tan \delta) - \chi \tau/\rho, \\ \partial_t b + \partial_x (\tilde{q}_b C u |u| - \tilde{q}_b k_1 \partial_x \eta - \tilde{q}_b k_2 \partial_x b) = 0, \end{cases} \quad (13)$$



where we identified  $\text{sgn}(v_b)$  as the  $\text{sgn}(\tau_{\text{eff}})$  and  $\chi = \begin{cases} 1 & \theta_c \geq \theta_{\text{eff}} \\ 0 & \text{otherwise} \end{cases}$ .

Regarding the stationary solutions of system (13), it is difficult to obtain an explicit expression in general. However, it is interesting to firstly analyze the simple case concerning lake at rest solution that is a steady solution for the Saint Venant system. That is, those ones verifying

$$b + h = \eta_0 \text{ constant}, \quad q = 0. \quad (14)$$

It is easy to check that they are also steady solutions of previous system if gravitational effects are not considered ( $k_1 = k_2 = 0$ ), since we recover  $\tau = 0$  and therefore  $\theta = 0$  and  $Q_b = 0$ . That means that solutions given by (14) are steady solutions independently of the sediment layer profile  $b(x)$ . Obviously, this is a limitation of classical models and non-physical solution will be kept.

On the contrary, this is not the case for the proposed model with gravitational effects. Actually, we have the following result.

**Proposition 1.** *Let  $\eta_0$  constant be the free surface level of a fluid at rest ( $u = 0$ ), with  $b(x)$  the sediment layer and  $\delta$  the angle of repose of the sediment. Then*

$$(\eta_0, 0, b(x)) \text{ is a steady solution} \quad \text{if and only if} \quad |\partial_x b| \leq \tan \delta.$$

*That is, a lake at rest solution is steady if and only if the sediment layer has a slope lower than the slope given by the angle of repose of the sediment.*

*Proof.* Let us start proving that the condition  $|\partial_x b| \leq \tan \delta$  is equivalent to  $\theta_{\text{eff}} \leq \theta_c$  under the hypothesis  $\partial_x \eta = 0, u = 0$ . In this case

$$\theta_{\text{eff}} = \frac{k_2 |\partial_x b|}{g(1/r - 1) d_s} = \frac{\vartheta g d_s (1/r - 1)}{g(1/r - 1) d_s} |\partial_x b| = \frac{\theta_c}{\tan \delta} |\partial_x b| \leq \theta_c,$$

and this inequality holds if and only if  $|\partial_x b| \leq \tan \delta$ .

Using the condition  $\theta_{\text{eff}} \leq \theta_c$ , it is easy to check that  $Q_b = h_m = 0$  (see (7) and (8)), and therefore  $\partial_t \eta = \partial_t q = \partial_t b = 0$ , i.e.,  $(\eta_0, 0, b(x))$  is a steady solution.

Assuming now that  $(\eta_0, 0, b(x))$  is a steady solution, we obtain

$$\partial_x (k_2 \tilde{q}_b \partial_x b) = 0 \quad \text{and} \quad h_m (\partial_x b + \text{sgn}(v_b) \tan \delta) = 0.$$

From the first condition, either  $\partial_x b = 0$  and therefore  $\tau_{\text{eff}} = 0 = \theta_{\text{eff}} \leq \theta_c$  and also  $h_m = 0$ , or  $\tilde{q}_b = 0$  and therefore  $(\theta_{\text{eff}} - \theta_c)_+ = 0$ , which ends the proof.  $\square$

Let us now study steady solutions in the general case, neglecting the friction term  $\chi \tau / \rho$  in the momentum equation in (13).

**Theorem 1.** *Let  $(\eta(x), q_0, b(x))$  be the values of the free surface, discharge and sediment layer satisfying that  $Q_b = 0$ , with  $q_0$  constant. Then, it is a steady solution of system (13) if and only if it satisfies*

$$- \text{sgn}(\tau_{\text{eff}}) \beta \partial_x b \leq \tan \delta \left( 1 - \frac{\text{sgn}(\tau_{\text{eff}}) C |q_0| q_0}{g d_s \theta_c (1/r - 1)} \frac{1}{(\eta - b)^2} \right), \quad \partial_x \eta = \alpha \partial_x b, \quad (15)$$

with

$$\alpha = \frac{-q_0^2}{g(\eta - b)^3 - q_0^2} \quad \text{and} \quad \beta = 1 + \frac{\alpha}{(1/r - 1)}.$$

*Proof.* Let us start by noticing that the steady solutions of system (13) with no sediment transport are given by

$$\partial_x q = 0, \quad \partial_x \left( \frac{u^2}{2} + g\eta \right) = 0, \quad Q_b = 0. \quad (16)$$

The first condition implies that  $q(x) = q_0$  constant. From the second condition in (16), and writing  $u$  as  $q_0/(\eta - b)$ , we deduce that

$$\partial_x \eta = \alpha \partial_x b, \quad \text{with } \alpha = \frac{-q_0^2}{g(\eta - b)^3 - q_0^2}.$$

Furthermore, since  $Q_b = 0$ , the only possibility is that  $\theta_{\text{eff}} \leq \theta_c$  holds, which leads to the inequality

$$\left| \frac{\tan \delta C |u| u}{gd_s \theta_c (1/r - 1)} - \beta \partial_x b \right| \leq \tan \delta, \quad \text{where } \beta = 1 + \frac{\alpha}{(1/r - 1)}. \quad (17)$$

Now, we can solve the inequality for the unknown  $\partial_x b$ , taking into account that the sign of the left hand side coincides with  $\text{sgn}(\tau_{\text{eff}})$ , obtaining inequality (15), which ends the proof.  $\square$

Notice that the Proposition 1 is a particular case of the Theorem 1 where  $q_0 = 0$ , obtaining  $\alpha = 0$  and  $\beta = 1$  in (17) and  $\eta(x) = \eta_0$  constant.

When the limit case is considered in (15), i.e. when the equality holds, the explicit expressions of  $\eta$  and  $b$  are the solutions of the resulting nonlinear ODE system. Note that  $\eta, b$  in (15) can be also found by solving just the initial value problem for the sediment, and updating the free surface value at each step using conservation of the energy (middle condition in (16)), that is  $\eta = b + h$  where  $h$  is the greater root (for subcritical solutions) of the third-order degree polynomial  $2gh^3 + 2(gb - K_0)h^2 + q_0^2 = 0$ , where  $K_0 = u_0^2/2 + g\eta_0$ .

In the results presented in this subsection we have focused on the generalized Ashida-Michiue model for the sake of simplicity. However, many other Saint Venant Exner models including gravitational effects could be written in the same form as (12)-(13), for instance the generalized Meyer-Peter & Müller model defined by (10) for  $K = 8$ . In the next subsection other possible generalizations to include gravitational effects are discussed, which can be easily written under the form (12)-(13). Consequently, the same numerical technique that is proposed in Section 3 can be applied for this family of models.

## 2.4 A general formulation of bedload sediment transport models with gravitational effects

In this section we briefly present several approaches to include gravitational effects in classical models, and the relations between them. As we commented before, it is suitable for the development of the semi-implicit method presented in Section 3 if the model is written under the form (12). Thus, all the discussed models below will be expressed in the same way.

In classical models, with the purpose of including gravitational effects, we shall replace  $\tau$  with  $\tau_{\text{eff}}$  and  $\theta$  with  $\theta_{\text{eff}}$  in the solid transport discharge  $Q_b$ . For example, when considering the family of classical models defined by the solid transport discharge (4), the corresponding models with gravitational effects are defined by

$$\frac{Q_b}{Q} = \text{sgn}(\tau_{\text{eff}}) \frac{\alpha_1}{1 - \varphi} \theta_{\text{eff}}^{\beta_1} (\theta_{\text{eff}} - \alpha_2 \theta_c)_+^{\beta_2} \left( \sqrt{\theta_{\text{eff}}} - \alpha_3 \sqrt{\theta_c} \right)^{\beta_3},$$

being  $\alpha_1, \alpha_2, \alpha_3, \beta_1, \beta_2$  and  $\beta_3$  non-negative constants depending on each model.

In addition, note that the effective shear stress must be defined to write previous models under the form (12). Actually, a different family of bedload models is obtained for each definition of  $\tau_{\text{eff}}$  proposed in the literature.

In the next lines we present some relevant definitions of  $\tau_{\text{eff}}$  in order to show the differences and the similarities, but also to give a justification of our choice given in (6).

Let us begin with the effective shear stress introduced in Fowler *et al.* [19] that we denote by  $\tau_{\text{eff}}^F$  and which is given by

$$\frac{\tau_{\text{eff}}^F}{\rho} = \frac{\tau}{\rho} - \lambda g d_s (1/r - 1) \partial_x b, \quad (18)$$

where  $\tau$  is a quadratic law defined as in (2) and  $\lambda = 1$ . Later, Morales de Luna *et al.* [31] proposed to define  $\lambda = \vartheta$ , where  $\vartheta$  is defined in (6), with the aim of recovering lake at rest steady solutions associated to the repose angle of the sediment. Whatever the value of  $\lambda$ , we find a family of models that can be reformulated defining  $Q_b$  as in (12a), and  $\tilde{q}_b, k_1, k_2$  as follows

$$\tilde{q}_b = \frac{\rho Q}{|\tau_{\text{eff}}^F|} \frac{\alpha_1}{1 - \varphi} (\theta_{\text{eff}}^F)^{\beta_1} (\theta_{\text{eff}}^F - \alpha_2 \theta_c)^{\beta_2} \left( \sqrt{\theta_{\text{eff}}^F} - \alpha_3 \sqrt{\theta_c} \right)^{\beta_3}, \quad (19)$$

with

$$\theta_{\text{eff}}^F = \frac{|\tau_{\text{eff}}^F|/\rho}{(1/r - 1)g d_s}, \quad k_1 = 0 \quad \text{and} \quad k_2 = \lambda g d_s (1/r - 1).$$

Note that the definition of  $k_2$  is the same that in previous cases (12b), but  $k_1$  is neglected. This means that the free surface gradient has no influence on the solid transport discharge when  $\tau_{\text{eff}}^F$  is considered. Equivalently,  $\tau_{\text{eff}}$  in (6) matches with  $\tau_{\text{eff}}^F$  if the free surface of the fluid is constant,  $\partial_x(b + h) = 0$ .

Let us now go deeper in the definition of  $\tau_{\text{eff}}$  to understand the expression (6) that we use in this work. In Fernández-Nieto *et al.* [18] the Navier-Stokes system is asymptotically analyzed to deduce a Saint Venant Exner system, leading to propose several models including gravitational effects and satisfying a dissipative energy balance. These gravitational effects are included through the considered effective shear stress. The law considered for the drag force between the fluid and granular layers determines both the model and the effective shear stress. In particular, two expressions for the effective shear stress are deduced corresponding to a linear or quadratic friction law, denoted by  $\tau_{\text{eff}}^L$  or  $\tau_{\text{eff}}^Q$  respectively, that we present next.

In the linear friction case, it is defined by

$$\frac{\tau_{\text{eff}}^L}{\rho} = \frac{\vartheta d_s}{h_m} \frac{\tau^L}{\rho} - \frac{\vartheta g d_s}{r} \partial_x (rh + b), \quad \text{with} \quad \frac{\tau^L}{\rho} = \frac{C h_m u \sqrt{g(1/r - 1) d_s}}{\vartheta d_s}, \quad (20)$$

or equivalently,

$$\frac{\tau_{\text{eff}}^L}{\rho} = C u \sqrt{g(1/r - 1) d_s} - \frac{\vartheta g d_s}{r} \partial_x (rh + b). \quad (21)$$

Now the family of models is given by

$$Q_b = \frac{\tau_{\text{eff}}^L}{\rho} \tilde{q}_b = \tilde{q}_b (C u \sqrt{g(1/r - 1) d_s} - k_1 \partial_x (b + h) - k_2 \partial_x b), \quad (22)$$

where

$$\tilde{q}_b = \frac{\rho Q}{|\tau_{\text{eff}}^L|} \frac{\alpha_1}{1 - \varphi} (\theta_{\text{eff}}^L)^{\beta_1} (\theta_{\text{eff}}^L - \alpha_2 \theta_c)_+^{\beta_2} \left( \sqrt{\theta_{\text{eff}}^L} - \alpha_3 \sqrt{\theta_c} \right)^{\beta_3},$$

and with  $k_1$  and  $k_2$  as in (12b) for  $\theta_{\text{eff}}^L = \frac{|\tau_{\text{eff}}^L|/\rho}{(1/r-1)gd_s}$ .

In the quadratic friction case, the effective shear stress is (see [18])

$$\frac{\tau_{\text{eff}}^Q}{\rho} = gd_s(1/r - 1)|\Phi|\Phi, \quad (23)$$

where

$$\Phi = \text{sgn}(u) \frac{\sqrt{|\tau^Q|/\rho}}{\sqrt{(1/r - 1)gd_s}} - \sqrt{\left| \frac{\vartheta}{1 - r} \partial_x (rh + b) \right|} \text{sgn}(\partial_x (rh + b)),$$

with  $\tau^Q$  defined in terms of  $\tau$  (2) as

$$\tau^Q = \frac{h_m}{\vartheta d_s} \tau. \quad (24)$$

The effective shear stress  $\tau_{\text{eff}}^Q$  (23) gives other family of bedload models, where

$$\text{sgn}(\tau_{\text{eff}}^Q) = \text{sgn}(\Phi) \quad \text{and} \quad \theta_{\text{eff}}^Q = |\Phi|^2,$$

which can be reformulated under a similar expression to (12a), concretely we obtain

$$Q_b = \tilde{q}_b \left( u \sqrt{\frac{\vartheta d_s}{h_m}} C - k_1 \partial_x (b + h) - k_2 \partial_x b \right), \quad (25a)$$

with

$$\tilde{q}_b = \frac{Q}{\left| u \sqrt{\frac{\vartheta d_s}{h_m}} C - k_1 \partial_x (b + h) - k_2 \partial_x b \right|} \frac{\alpha_1}{1 - \varphi} (\theta_{\text{eff}}^Q)^{\beta_1} (\theta_{\text{eff}}^Q - \alpha_2 \theta_c)_+^{\beta_2} \left( \sqrt{\theta_{\text{eff}}^Q} - \alpha_3 \sqrt{\theta_c} \right)^{\beta_3} \quad (25b)$$

and

$$k_1 = \frac{\sqrt{\vartheta gd_s r}}{\sqrt{|\partial_x (rh + b)|}}, \quad k_2 = \frac{\sqrt{\vartheta gd_s r}}{\sqrt{|\partial_x (rh + b)|}} (1/r - 1). \quad (25c)$$

Note that this model is much more complicate that any of the models defined by (19) or (22). Firstly, because the values  $k_1$ ,  $k_2$  are no more constant. Secondly, note that  $h_m$  can be defined by (7) or (9), in terms of  $(\theta_{\text{eff}}^Q - \theta_c)_+$ , and as a consequence  $\theta_{\text{eff}}^Q$  is implicitly defined.

Let us now make a comparison of the three definitions (18), (20) and (23) given for the effective shear stress. When the effective shear stress of the linear model (21) is compared with the definition (18) given by Fowler [19], two differences are observed. Firstly, the first term in the definition changes, it is quadratic in the velocity for the Fowler's model and linear in (21), which is consistent with the hypothesis of a linear drag force between fluid and sediment layer. Secondly, the gravitational terms are different, although they are equal when the free surface is constant and  $\lambda = \vartheta$ . It can be easily seen by writing

$$\frac{\vartheta gd_s}{r} \partial_x (rh + b) = \vartheta gd_s (1/r - 1) \partial_x b + \vartheta gd_s \partial_x (b + h).$$

Therefore, the definition of the gravitational effects introduced in [18] is more general, since it takes into account the weight of the upper fluid and the coupled effect of the variations of the free surface and sediment.

Furthermore, when looking at the effective shear stress deduced for the quadratic model (23) we do not find the same definition than in the Fowler's model, even if they both correspond to a quadratic friction law. Moreover the gravitational terms are also different, being much more complex in the quadratic model.

The effective shear stress (6) used in this work may be interpreted as a linearized version of the quadratic effective shear stress, corresponding to the definition  $\tau_{\text{eff}}^L$  (20) when the friction term  $\tau^L$  is replaced by  $\tau^Q$  defined in (24), thus obtaining our definition

$$\frac{\tau_{\text{eff}}}{\rho} = \frac{\tau}{\rho} - \frac{\vartheta g d_s}{r} \partial_x (rh + b).$$

As commented above, this model can be also seen as an enhanced Fowler's model where the gravitational effects take into account the free surface gradient.

Finally, the corresponding family of models for the proposed  $\tau_{\text{eff}}$  defined in (6) can be reformulated easily keeping  $Q_b$  as in (12a), that is,

$$Q_b = \frac{\tau_{\text{eff}}}{\rho} \tilde{q}_b = \tilde{q}_b (C |u| u - k_1 \partial_x (b + h) - k_2 \partial_x b),$$

but where  $\tilde{q}_b$  in (12c) is replaced with

$$\tilde{q}_b = \frac{\rho Q}{|\tau_{\text{eff}}|} \frac{\alpha_1}{1 - \varphi} \theta_{\text{eff}}^{\beta_1} (\theta_{\text{eff}} - \alpha_2 \theta_c)_+^{\beta_2} \left( \sqrt{\theta_{\text{eff}}} - \alpha_3 \sqrt{\theta_c} \right)^{\beta_3},$$

$k_1$  and  $k_2$  taken the same values introduced in (12b).

### 3 Semi-implicit approach

We are interested in this work on the large-time scale, i.e., very slow processes where the characteristic time associated to the sediment is very large, and usually the fluid-sediment interaction is weak. This is the case for example of the movement of a dune in a river or a lake. In these situations it is common to have subcritical regimes. Furthermore, note that second order space derivatives of the free surface and the sediment layer appear in system (13). Then, when discretizing it using an explicit scheme it leads to a very restrictive stability condition (CFL) and therefore to a huge computational cost because of the small time-steps.

In this section, we develop an efficient semi-implicit numerical scheme to relax the CFL condition by removing the gravitational contributions, which can be applied to any model with gravitational effect written under formulation (12) –or (25)– and (13). The spatial and time discretizations are described through the finite volume method.

Let us start with the spatial discretization, where we consider a uniform mesh step  $\Delta x$  without loss of generality. Then, we subdivide the computational domain into control volumes denoted by  $V_i = (x_{i-1/2}, x_{i+1/2})$  with center  $x_i = (x_{i-1/2} + x_{i+1/2}) / 2$ , for  $i \in \mathcal{I}$ , with  $\#(\mathcal{I}) = M$ . We consider a staggered mesh, that is, the discrete free surface and sediment variables  $(\eta_i, b_i)$  are defined at the center of the control volumes  $(x_i)$ , whereas the discrete discharge values  $(q_{i+1/2})$  are at the interfaces  $(x_{i+1/2})$ . This C-grid staggering has the advantage that the linear system resulting from the semi-implicit time discretization is more compact.

We propose to discretize system (12), (13) using the semi-implicit scheme introduced in [11, 10, 8] based on the theta method. This strategy allows us to remove the celerity contribution to the CFL condition. Thus, defining  $h_i = \eta_i - b_i$ ,  $u_i = (q_{i-1/2} + q_{i+1/2})/h_i$  and the Courant numbers

$$C_{vel} = \frac{\Delta t}{\Delta x} \max_{i \in \mathcal{I}} |u_i|, \quad C_{cel} = \frac{\Delta t}{\Delta x} \max_{i \in \mathcal{I}} (|u_i| + \sqrt{gh_i}),$$

with  $\Delta t$  the time step, the explicit method has a stability restriction that can be approximated by  $C_{cel} < 1$ , whereas the semi-implicit method relaxes this condition to  $C_{vel} < 1$ . Therefore, in subcritical regime ( $|u|/\sqrt{gh} \ll 1$ ) this approach allows us to give larger time steps since the restrictive contribution is the gravitational one.

The theta method (hereinafter  $\Theta$ -method) reads

$$w^{n+1} = w^n + \Delta t \Theta f(t^{n+1}, w^{n+1}) + \Delta t (1 - \Theta) f(t^n, w^n),$$

for an arbitrary ODE system  $w' = f(t, w)$ , being  $\Theta \in [0, 1]$  the implicitness parameter. Note that in the limit cases  $\Theta = 0$  and  $\Theta = 1$ , the explicit and implicit Euler methods are recovered. As expected, this method is more diffusive for large values of  $\Theta$ . In practice, we choose  $\Theta$  slightly larger than  $1/2$ , since this method is unconditionally stable for  $\Theta \in [1/2, 1]$ .

Since the goal of this work is not to propose high order semi-implicit scheme, we perform a discretization based on the theta method, which is first order accurate (second order if  $\Theta = 1/2$ , Crank-Nicolson method). This procedure can be adapted to more accurate time discretizations if needed via an IMEX-ARK (Implicit Explicit Additive Runge Kutta) methods (see [27]), following the description made in [5, 23].

In the following we describe how the system (13) is discretized. The key point is considering all the convective terms in a explicit way, while terms involving the derivative of the free surface ( $\partial_x \eta$ ) and the sediment layer ( $\partial_x b$ ) are discretized using the semi-implicit method. Firstly, the discrete momentum equation is written as

$$\begin{aligned} q_{i+1/2}^{n+1} &= G_{i+1/2}^n - \frac{\Delta t}{\Delta x} g \Theta (h + C h_m)_{i+1/2}^n (\eta_{i+1}^{n+1} - \eta_i^{n+1}) \\ &\quad - \frac{\Delta t}{\Delta x} g \Theta (1/r - 1) C_{i+1/2}^n h_{m,i+1/2}^n (b_{i+1}^{n+1} - b_i^{n+1}), \end{aligned} \quad (26)$$

defining as  $h_{i+1/2}$  the upwind value depending on  $q_{i+1/2}$  (see [25, 5] for instance). In previous equation  $G_{i+1/2}^n$  collects the explicit terms:

$$\begin{aligned} G_{i+1/2} &= q_{i+1/2} - \frac{\Delta t}{\Delta x} \left( \Delta x \partial_x (q^2/h)_{i+1/2} + g (1 - \Theta) (h + C h_m)_{i+1/2} (\eta_{i+1} - \eta_i) \right. \\ &\quad \left. + g (1 - \Theta) (1/r - 1) C h_{m,i+1/2} (b_{i+1} - b_i) \right) - \Delta t g (1/r - 1) h_{m,i+1/2} \text{sgn}(v_{b,i+1/2}) \tan \delta \\ &\quad - \Delta t \chi_{i+1/2}^n C_{i+1/2}^n |u_{i+1/2}^n| u_{i+1/2}^n. \end{aligned}$$

For the sake of simplicity, we employ an upstream first order finite difference approximation for the advection term

$$\Delta x \partial_x (q^2/h)_{i+1/2} = \begin{cases} (qu)_{i+\frac{1}{2}} - (qu)_{i-\frac{1}{2}} & \text{if } u_{i+\frac{1}{2}} > 0, \\ (qu)_{i+\frac{3}{2}} - (qu)_{i+\frac{1}{2}} & \text{if } u_{i+\frac{1}{2}} < 0, \end{cases}$$

where  $u_{i+1/2} = q_{i+1/2}/h_{i+1/2}$ . Any other high order approximation could be used to increase the order of the method if required.

Next, the continuity and the sediment evolution equations are discretized as

$$\begin{aligned}
\Delta x \eta_i^{n+1} &= \Delta x \eta_i^n - \Delta t \Theta \left( q_{i+1/2}^{n+1} - q_{i-1/2}^{n+1} \right) - \Delta t (1 - \Theta) \left( q_{i+1/2}^n - q_{i-1/2}^n \right) \\
&- \Delta t \left( \tilde{q}_{b_{i+1/2}}^n C_{i+1/2}^n \left| u_{i+1/2}^n \right| u_{i+1/2}^n - \tilde{q}_{b_{i-1/2}}^n C_{i-1/2}^n \left| u_{i-1/2}^n \right| u_{i-1/2}^n \right) \\
&+ \Theta \frac{\Delta t}{\Delta x} \left( \tilde{q}_{b_{i+1/2}}^n \left( k_1 (\eta_{i+1}^{n+1} - \eta_i^{n+1}) + k_2 (b_{i+1}^{n+1} - b_i^{n+1}) \right) \right. \\
&\quad \left. - \tilde{q}_{b_{i-1/2}}^n \left( k_1 (\eta_i^{n+1} - \eta_{i-1}^{n+1}) + k_2 (b_i^{n+1} - b_{i-1}^{n+1}) \right) \right) \\
&+ (1 - \Theta) \frac{\Delta t}{\Delta x} \left( \tilde{q}_{b_{i+1/2}}^n \left( k_1 (\eta_{i+1}^n - \eta_i^n) + k_2 (b_{i+1}^n - b_i^n) \right) \right. \\
&\quad \left. - \tilde{q}_{b_{i-1/2}}^n \left( k_1 (\eta_i^n - \eta_{i-1}^n) + k_2 (b_i^n - b_{i-1}^n) \right) \right), \tag{27}
\end{aligned}$$

and

$$\begin{aligned}
\Delta x b_i^{n+1} &= \Delta x b_i^n - \Delta t \left( \tilde{q}_{b_{i+1/2}}^n C_{i+1/2}^n \left| u_{i+1/2}^n \right| u_{i+1/2}^n - \tilde{q}_{b_{i-1/2}}^n C_{i-1/2}^n \left| u_{i-1/2}^n \right| u_{i-1/2}^n \right) \\
&+ \Theta \frac{\Delta t}{\Delta x} \left( \tilde{q}_{b_{i+1/2}}^n \left( k_1 (\eta_{i+1}^{n+1} - \eta_i^{n+1}) + k_2 (b_{i+1}^{n+1} - b_i^{n+1}) \right) \right. \\
&\quad \left. - \tilde{q}_{b_{i-1/2}}^n \left( k_1 (\eta_i^{n+1} - \eta_{i-1}^{n+1}) + k_2 (b_i^{n+1} - b_{i-1}^{n+1}) \right) \right) \\
&+ (1 - \Theta) \frac{\Delta t}{\Delta x} \left( \tilde{q}_{b_{i+1/2}}^n \left( k_1 (\eta_{i+1}^n - \eta_i^n) + k_2 (b_{i+1}^n - b_i^n) \right) \right. \\
&\quad \left. - \tilde{q}_{b_{i-1/2}}^n \left( k_1 (\eta_i^n - \eta_{i-1}^n) + k_2 (b_i^n - b_{i-1}^n) \right) \right). \tag{28}
\end{aligned}$$

Now, the values of  $q_{i+1/2}^{n+1}$  (26) are embedded into (27), and we obtain from (27) and (28) a linear system with  $2M$  equations and unknowns  $(\eta_i, b_i)$ ,  $i \in \mathcal{I}$ . To solve it, we slip it into two linear system  $M \times M$ , one for the free surface values  $\eta_i^{n+1}$  where the terms in  $b^{n+1}$  are moved to the right hand side term of the system, and vice versa for the system whose unknowns are  $b_i^{n+1}$ , and then an iterative method is applied. Note that this strategy is no more than the block Gauss-Seidel algorithm. Let us describe in detail the method.

We consider the sequence  $\left\{ \eta_i^{n,k}, b_i^{n,k} \right\}_{i \in \mathcal{I}}^{k \in \mathbb{N}}$  with  $\eta_i^{n,0} = \eta_i^n$  and  $b_i^{n,0} = b_i^n$  for  $i \in \mathcal{I}$ . For the free surface values, we have the system

$$-A_{i-1/2} \eta_{i-1}^{n,k+1} + \left( \Delta x + A_{i-1/2}^n + A_{i+1/2}^n \right) \eta_i^{n,k+1} - A_{i+1/2}^n \eta_{i+1}^{n,k+1} = \mathcal{H}_i^n + f_{1,i}^{n,k}, \tag{29}$$

with

$$\begin{aligned}
A_{i+1/2} &= g \frac{\Theta^2 \Delta t^2}{\Delta x} (h + C h_m)_{i+1/2} + k_1 \frac{\Theta \Delta t}{\Delta x} \tilde{q}_{b_{i+1/2}}, \\
\mathcal{H}_i &= \Delta x \eta_i - \Delta t \Theta \left( G_{i+1/2} - G_{i-1/2} \right) - \Delta t (1 - \Theta) \left( q_{i+1/2} - q_{i-1/2} \right) \\
&- \Delta t \left( \tilde{q}_{b_{i+1/2}}^n C_{i+1/2}^n \left| u_{i+1/2}^n \right| u_{i+1/2}^n - \tilde{q}_{b_{i-1/2}}^n C_{i-1/2}^n \left| u_{i-1/2}^n \right| u_{i-1/2}^n \right) \\
&+ (1 - \Theta) \frac{\Delta t}{\Delta x} \left( \tilde{q}_{b_{i+1/2}}^n \left( k_1 (\eta_{i+1} - \eta_i) + k_2 (b_{i+1} - b_i) \right) \right. \\
&\quad \left. - \tilde{q}_{b_{i-1/2}}^n \left( k_1 (\eta_i - \eta_{i-1}) + k_2 (b_i - b_{i-1}) \right) \right),
\end{aligned}$$

and

$$\begin{aligned} f_{1,i}^{n,k} &= k_2 \frac{\Theta \Delta t}{\Delta x} \left( \tilde{q}_{b_{i+1/2}}^n (b_{i+1}^{n,k} - b_i^{n,k}) - \tilde{q}_{b_{i-1/2}}^n (b_i^{n,k} - b_{i-1}^{n,k}) \right) \\ &+ g(1/r - 1) \frac{\Theta^2 \Delta t^2}{\Delta x} \left( (C h_m)_{i+1/2}^n (b_{i+1}^{n,k} - b_i^{n,k}) - (C h_m)_{i-1/2}^n (b_i^{n,k} - b_{i-1}^{n,k}) \right). \end{aligned}$$

Analogously, for the sediment values, we obtain

$$-B_{i-1/2} b_{i-1}^{n,k+1} + \left( \Delta x + B_{i-1/2}^n + b_{i+1/2}^n \right) b_i^{n,k+1} - B_{i+1/2}^n b_{i+1}^{n,k+1} = \mathcal{L}_i^n + f_{2,i}^{n,k} \quad (30)$$

with

$$\begin{aligned} B_{i+1/2} &= k_2 \frac{\Theta \Delta t}{\Delta x} \tilde{q}_{b_{i+1/2}}, \\ \mathcal{L}_i &= \Delta x b_i - \Delta t \left( \tilde{q}_{b_{i+1/2}} C_{i+1/2}^n |u_{i+1/2}| u_{i+1/2} - \tilde{q}_{b_{i-1/2}} C_{i-1/2}^n |u_{i-1/2}| u_{i-1/2} \right) \\ &+ (1 - \Theta) \frac{\Delta t}{\Delta x} \left( \tilde{q}_{b_{i+1/2}} (k_1 (\eta_{i+1} - \eta_i) + k_2 (b_{i+1} - b_i)) \right. \\ &\quad \left. - \tilde{q}_{b_{i-1/2}} (k_1 (\eta_i - \eta_{i-1}) + k_2 (b_i - b_{i-1})) \right), \end{aligned}$$

and

$$f_{2,i}^{n,k} = k_1 \frac{\Theta \Delta t}{\Delta x} \left( \tilde{q}_{b_{i+1/2}}^n (\eta_{i+1}^{n,k} - \eta_i^{n,k}) - \tilde{q}_{b_{i-1/2}}^n (\eta_i^{n,k} - \eta_{i-1}^{n,k}) \right).$$

Note that the linear systems (29),(30) are tridiagonal systems, whose associated matrix is a symmetric strictly diagonally dominant matrix, which can be solved using the Thomas' algorithm.

The Gauss-Seidel algorithm is then applied as follows:

- System (29) is solved to find the new free surface values  $\eta_i^{n,k+1}$ .
- The values of the sediment  $b_i^{n,k+1}$  are found solving system (30), using  $f_{2,i}^{n,k+1}$  with the updated values  $\eta_i^{n,k+1}$  instead of  $f_{2,i}^{n,k}$  in the right hand side.
- This procedure continues until convergence, that occurs when

$$\text{error} = \max\{ \|\eta^{n,k+1} - \eta^{n,k}\|_1^{\mathcal{I}}, \|b^{n,k+1} - b^{n,k}\|_1^{\mathcal{I}}, \} < \text{tolerance}$$

or  $k$  equals the number maximum of iterations.

Finally, the new values of  $q_{i+1/2}^{n+1}$  are updated using (26). Let us remark that in practice we do not need more than 2-3 iterations since the values  $\tilde{q}_b$  are usually small. If these contributions grows up, we would need some more iterations of the Gauss-Seidel algorithm to reach the convergence. Note also that for models defined by the family (19), for which  $k_1 = 0$ , the system (30) for  $b_i^{n+1}$  is exactly solved and by replacing it in (27) the new states  $\eta_i^{n+1}$  are found. Therefore, a single iteration is necessary.

**Remark 2.** Regarding the boundary conditions, we consider either wall or subcritical boundary conditions, and they are imposed as usually in these semi-implicit schemes.

For the wall condition, we fix  $q_{1/2} = q_{M+1/2} = 0$  and for  $\eta, b$  a ghost cell technique is used, defining  $\eta_0 = \eta_1$ ,  $b_0 = b_1$  and the same for the right boundary.

In the case of subcritical conditions, the discharge is fixed upstream  $q_{1/2} = q_{ext}$ , downstream we use a ghost cell and fix the free surface value  $\eta_M = \eta_{ext}$  and the bottom is duplicated  $b_M = b_{M-1}$ . Let us remark that in case of subcritical boundary conditions, the matrix of the linear system and the right hand side should be accordingly modified (see e.g. [34]).



## 4 Numerical results

Some results are presented in this section to show that the proposed semi-implicit method is indeed efficient. In principle, we could consider any of the models presented in Subsection 2.4. For the sake of simplicity, in the numerical tests we only focus on the generalization of the Ashida-Michiue model given by (8) with  $K_e/K_d = 17$ .

The implicitness parameter has been set to  $\Theta = 0.55$  in all the tests. When errors are measured, the reference solution is computed with an explicit code corresponding with a third-order Runge-Kutta method (RK3), where the time step is adaptive according to a low fixed Courant number  $C_{cel} = 0.1$ . However, with the semi-implicit approach the time step  $\Delta t$  is fixed and compute the maximum Courant numbers achieved. We also measure the speed-up reached for all the tests. The computational times showed here have been measured on a PC with Intel®Core i7-7700HQ and 16 GB of RAM.

### 4.1 Steady lake-at-rest solutions

As commented in Section 2.3, one of the drawback of models without gravitational effects is the fact that they keep non-physical steady solutions in the lake at rest configuration (14). In Theorem 1 we establish the condition to be steady solution in this configuration for the proposed model. In this subsection we check numerically that this property is satisfied.

To this end, we consider a fluid and sediment with the properties given in Table 1 where we have fixed  $\delta_0 = 3^\circ, 15^\circ, 25^\circ, 45^\circ, 75^\circ$ . We consider a computational domain  $[0 \text{ m}, 10 \text{ m}]$  discretized

$n$	$\theta_c$	$\rho/\rho_s$	$\varphi$	$d_s \text{ (mm)}$	$\tan \delta$
0.01	0.047	0.34	0.9	1.0	$\tan \delta_0$

Table 1: *Material properties for test 4.1.*

using 800 points and wall boundary conditions. A lake at rest configuration with initial conditions  $\eta_0(x) = 1 \text{ m}$ ,  $q_0(x) = 0 \text{ m}^2/\text{s}$  is taken. The sediment layer profile is given by a discontinuous step profile as follows

$$b_0(x) = \begin{cases} 0.2 \text{ m} & \text{if } 4 \text{ m} < x < 6 \text{ m} \\ 0.1 \text{ m} & \text{otherwise.} \end{cases}$$

This is a steady solution for the models without gravitational effects, whereas it is not for the model including these effects, as we check in Figure 2. Moreover, we see that the solution becomes steady when  $|\partial_x b|$  equals  $\tan \delta_0$ , as stated in Theorem 1.

In Table 2 the Courant numbers and speed-ups are shown for the simulations for the different values of  $\delta_0$ . We observe that for lower values of the angle of repose, the  $C_{cel}$  must be also smaller in order to not seeing spurious oscillations in the results. We see that high values of  $C_{cel}$  and speed-ups are achieved, thus the proposed method is much more computationally cheaper than the explicit method without loss of accuracy in the steady solutions. This is an expected result for this test since the velocity is very small.

### 4.2 Steady states for subcritical flows

In previous section we have dealt with lake-at-rest solutions analyzing the influence of the repose angle of the sediment. We focus here on some steady solutions given by Proposition 1, in particular in the limit case, where the equality holds. We will see that convective terms allow us to obtain steady solutions where the sediment is at rest but its slope is greater than the angle of repose

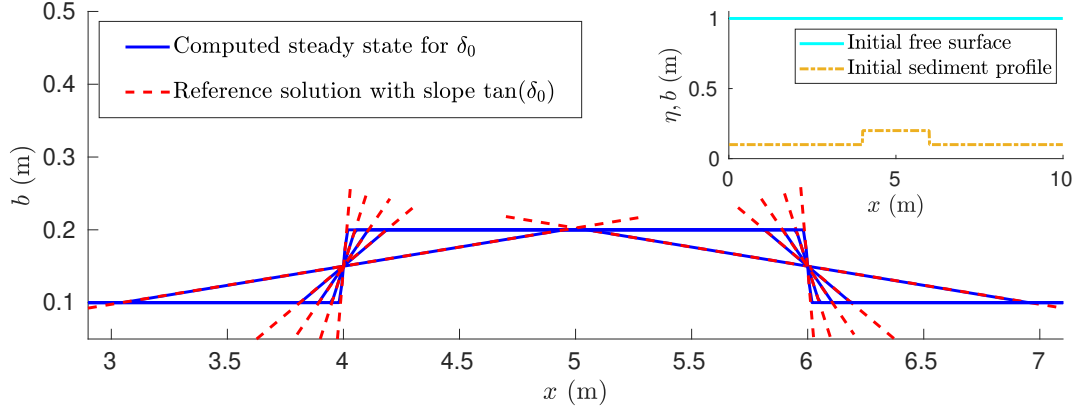


Figure 2: *Test 4.1. Sediment layer at steady state for values of  $\delta_0 = 3^\circ, 15^\circ, 25^\circ, 45^\circ, 75^\circ$ . Solid blue lines are the computed solutions and dashed lines are reference straight lines with the theoretical solutions. Inset figure: Initial profiles of the free surface (cyan solid line) and the sediment (dash-dotted brown line).*

$\delta_0(^{\circ})$	$\Delta t$ (s)/ $C_{cel}$ $\Theta$ -method	$C_{cel}$ RK3	Comp. time (s) $\Theta$ -method	Comp. time (min) RK3	Speed-up
3	0.05/11.9	0.4	48.3 (0.81 min)	29.6	36.8
15	0.1/23.8	0.8	24.1 (0.40 min)	15.3	38.1
25	0.3/71.3	0.8	7.8 (0.13 min)	15.1	116.4
45	0.5/118.9	0.9	4.7 (0.08 min)	14.2	180.9
75	1.5/356.5	0.9	1.6 (0.03 min)	14.3	539.1

Table 2: *Test 4.1. Speed-ups and Courant numbers and speed-ups achieved reached at time  $t_f = 10000$  s with the  $\Theta$ -method for the different values of  $\delta_0$ .*

of the material. This happens because convective terms in the effective Shields parameter are in equilibrium with the gravitational effects. In this case, we consider as material properties given in Table 3.

$n$	$\theta_c$	$\rho/\rho_s$	$\varphi$	$d_s$ (mm)	$\tan \delta$
0.02	0.047	1000/1540	0.9	3.2	$\tan 25^\circ$

Table 3: *Material properties for test 4.2.*

We take  $x \in [0 \text{ m}, 3 \text{ m}]$  and 300 points for its discretization, and the initial conditions given by

$$\eta_0(x) = 10 \text{ m}, \quad b_0(x) = \begin{cases} 1 \text{ m} & \text{if } 0.5 \text{ m} < x < 1 \text{ m} \\ 0 \text{ m} & \text{otherwise,} \end{cases}$$

and  $q_0(x) = q_0 \text{ m}^2/\text{s}$  with  $q_0 \in \mathbb{R}$  a constant. Subcritical boundary conditions (see Remark 2) are considered here, with  $q_{ext} = q_0 \text{ m}^2/\text{s}$  at the inlet and  $\eta_{ext} = 10 \text{ m}$  at the outlet boundaries. We allow

the flow evolve until the steady solution is reached. To this end, we consider that the steady state is reached when  $v_b < 10^{-4} \text{ m/s}$  everywhere. We take several values for the initial and boundary discharge,  $q_0 = 0, 0.8, 1.8, 3.8, 4.8$  and  $5.8 \text{ m}^2/\text{s}$ , including the lake at rest case ( $q_0 = 0 \text{ m}^2/\text{s}$ ). We fix the discharge such that  $\theta_{\text{eff}} < \theta_c$  where the bottom is flat in order to not having erosion processes. Otherwise, a steady state is reached, although it is different from the computed in (16) when the equality holds. Note that we have a inequality, so any solution verifying it will be a steady solution, whereas we are computing the limit case.

We observe that larger values of  $q_0$  need more time of simulation ( $t_{ST}$ ) to reach the steady state, as showed in Table 4. We see that very large times ( $t_{ST} \sim 10^5 \text{ s}$ ) are needed to reach the steady state. Let us remark that we compute an approximation of  $t_{ST}$  since our interest is to show an estimation and its evolution in terms of  $q_0$ . We see in this table that high Courant number are achieved ( $C_{cel} \approx 30$ ), allowing us to notably reduce the computational time.

$q_0 \text{ (m}^2/\text{s)}$	$t_{ST} \times 10^5 \text{ (s)}$	$\Delta t \text{ (s)}$	$C_{cel}$	Comp. time (min)
0.0	2.85	0.041	40.6	10.92
0.8	2.75	0.11	109.8	4.11
1.8	2.50	0.032	32.3	13.84
3.8	1.50	0.029	29.8	14.43
4.8	1.15	0.028	29.1	14.63
5.8	0.85	0.028	29.4	14.47

Table 4: *Test 4.2. Approximated time to reach the steady states ( $t_{ST}$ ), Courant numbers and computational times at final time  $t_f = 285000 \text{ s}$  ( $\approx 79 \text{ hours}$ ) with the  $\Theta$ -method for the different values of  $q_0$ .*

Figure 3 shows the steady states for different values of the initial discharge  $q_0$ , together with the computed analytical solutions, for both the sediment and the free surface. We see a good agreement between the computed and the analytical solutions in all the cases. We also observe in this figure how the balance between convective and gravitational contributions is acting. Concretely, increasing the velocity we obtain steady states where the slope of the sediment is far away from the angle of repose of the sediment (solution for  $q_0 = 0 \text{ m}^2/\text{s}$ ). In addition, the free surface is no more constant, although the deviation from a constant value is small (larger for larger values of  $q_0$ ).

### 4.3 Dune test

In this test we take a rectangular dune, which is swept along by the current. As material properties, we take the same as previous subsection, but letting the angle of repose vary,  $\tan \delta = \tan \delta_0$ , with  $\delta_0 = 3^\circ, 15^\circ, 25^\circ, 45^\circ, 75^\circ$ . As computational domain we take  $[0 \text{ m}, 1000 \text{ m}]$  discretized with 500 nodes. The initial conditions are given by

$$\eta_0(x) = 15 \text{ m}, \quad q_0(x) = 15 \text{ m}^2/\text{s} \quad \text{and} \quad b_0(x) = \begin{cases} 1.1 \text{ m} & \text{if } 200 \text{ m} < x < 400 \text{ m} \\ 0.1 \text{ m} & \text{otherwise.} \end{cases}$$

As in the previous test, we use subcritical boundary conditions, with  $q_{ext} = 15 \text{ m}^2/\text{s}$  at  $x = 0 \text{ m}$  and  $\eta_{ext} = 15 \text{ m}$  at  $x = 1000 \text{ m}$ . As final time we take  $t = 1209600 \text{ s}$  (14 days).

The evolution of the free surface and the sediment until final time for a fixed repose angle  $\delta_0 = 45^\circ$  and  $\Delta t = 2 \text{ s}$  ( $C_{cel} \approx 13.1$ ) is shown in Figure 4. We also show here the solution obtained if a semi-analytic approach is considered for system (13). It consists of considering that

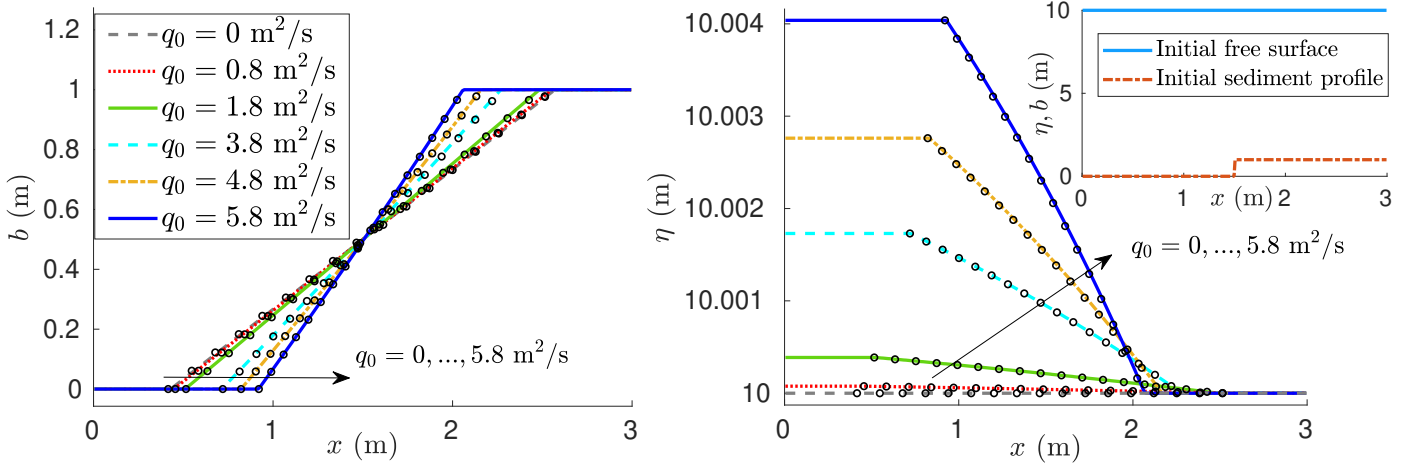


Figure 3: *Test 4.2. Sediment layer (left) and free surface (right) at steady state for different values of  $q_0$ . Lines are computed solutions and symbols analytic solutions given by (15). Inset figure: Initial profiles of the free surface (blue solid line) and sediment layer (dash-dotted brown line).*

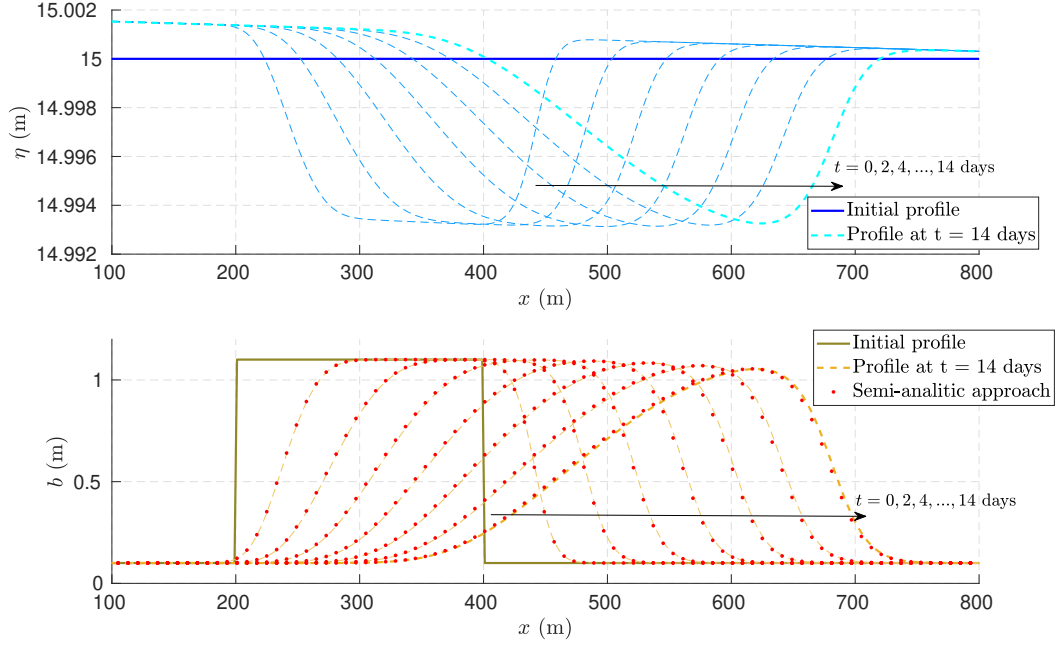


Figure 4: *Test 4.3. Evolution of the free surface (top figure) and the sediment layer (bottom figure) for  $\delta_0 = 45^\circ$  at times  $t = 0, 2, 4, \dots, 14$  days, with the  $\Theta$ -method and  $\Delta t = 2$  s ( $C_{cel} \approx 13.1$ ). Solid lines are the initial conditions and dashed lines are solutions at several times. Red dots are the solution obtained using the semi-analytic approach for  $\eta, q$  constant values.*

both the free surface and the discharge are constant values along the time,  $\eta(x, t) = \eta_0(x)$  and  $q(x, t) = q_0(x)$ , and using these values in the Exner equation  $\partial_t b + \partial_x Q_b = 0$  to find  $b(x, t)$ . This

will be a reasonable approximation of  $b$  as long as the free surface and the discharge are close to a constant value. Note that neither the height  $h(x, t)$  nor the velocity  $u(x, t)$  are constant with this approach. In the case showed in Figure 4, there are small perturbations of the free surface, and therefore this semi-analytic approach gives a good approximation of the sediment evolution.

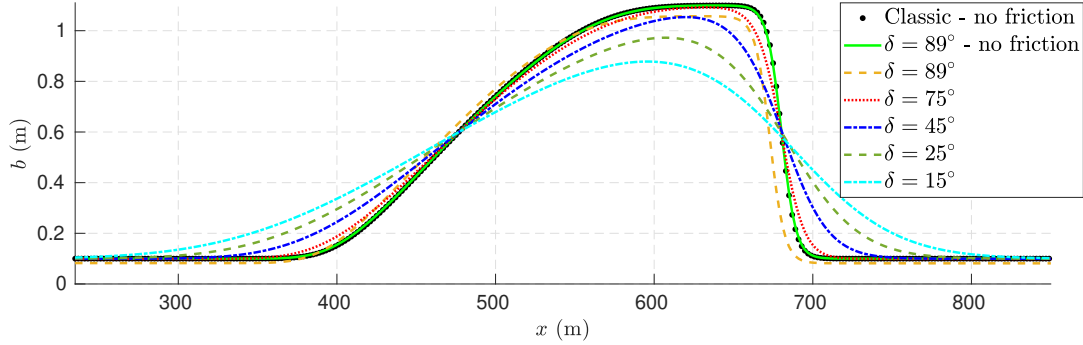


Figure 5: *Test 4.3. Sediment layer at steady state for several values of the angle of repose of the sediment. Classic model means model without gravitational effects and lines denoted by “no friction” are the solutions of the resulting system by neglecting the friction term, taking  $C = 0$  just in the momentum equation in (13).*

Figure 5 shows the solution at the final time  $t = 14$  days for different values of  $\delta_0$ . The solution of the classic model (removing gravitational effect and the friction term related to  $h_m$  in the momentum equation in (13)) is also showed. We see that when the angle of repose get lower, and therefore the gravitational effects get larger, the advancing front of the dune does not exhibit a straight shape but a smooth profile.

$\Delta t$ (s)	$C_{cel}$	$C_{vel}$	$Err_\eta [l_2/l_\infty]$ ( $\times 10^{-9}$ )	$Err_b [l_2/l_\infty]$ ( $\times 10^{-6}$ )	$Err_u [l_2/l_\infty]$ ( $\times 10^{-7}$ )
0.5	3.3	0.27	0.5/1.7	2.1/3.0	0.7/2.2
1.0	6.5	0.54	1.0/3.5	4.3/6.1	1.4/4.6
1.5	9.8	0.81	1.5/2.0	6.5/9.3	2.1/6.9
2.0	13.1	1.1	2.0/7.1	8.7/12.4	2.8/9.3
2.5	16.4	1.3	2.5/8.9	10.9/15.6	3.4/11.6
3.0	19.7	1.6	3.0/10.6	13.1/18.7	4.1/13.9

Table 5: *Test 4.3. Relative errors with respect to the explicit RK3 with  $C_{cel} = 0.1$ , and Courant numbers reached at  $t_f = 14$  days by the semi-implicit method, for the case  $\delta_0 = 45^\circ$ .*

The relative errors achieved by the semi-implicit method for different Courant numbers at final time  $t_f$ , for a fixed angle of repose  $\delta_0 = 45^\circ$ , are in Table 5. We see that very high Courant number  $C_{cel}$  can be used without losing the accuracy significantly. In Table 6 the speed-ups are shown. We see a speed-up 20 with the proposed method, leading to a large decreasing on the computational efforts. Let us remark that in practice we can get larger Courant number since the conditions of this test are quite smooth. For instance, we can run a simulation with  $C_{cel} = 18000$  and it remains stable despite of violating the condition based on  $C_{vel}$  by far.

Method	$\Delta t$ (s)	$C_{cel}$	Comp. time (s)	Speed-up
RK3	-	1.0	1425.7 (23.8 min)	1
$\Theta$ -method	0.5	3.3	368.14 (6.1 min)	3.9
$\Theta$ -method	1	6.5	187.73 (3.1 min)	7.6
$\Theta$ -method	1.5	9.8	134.55 (2.2 min)	10.6
$\Theta$ -method	2	13.1	106.82 (1.8 min)	13.3
$\Theta$ -method	2.5	16.4	85.20 (1.4 min)	16.7
$\Theta$ -method	3	19.7	71.29 (1.2 min)	20.0

Table 6: *Test 4.3. Speed-ups reached at final time  $t_f = 14$  days with the proposed semi-implicit method, for the case  $\delta_0 = 45^\circ$ .*

#### 4.4 Erosion coast process by a tidal force

In this last test we simulate the erosion in the mouth of a river, as an application of sediment transport problems to very slow processes, with a small characteristic time and a huge computational effort because of the long-time simulation.

As computational domain we take  $[0 \text{ m}, 25000 \text{ m}]$  with  $\Delta x = 25 \text{ m}$ . The material properties are taken as in Subsection 4.2, except for the manning coefficient, which is set as  $n = 0.018$ .

The initial condition are given by  $\eta_0(x) = 15 \text{ m}$ ,  $b_0(x) = 0.1 \text{ m}$  and  $q_0(x) = 8.1 \text{ m}^2/\text{s}$ . Here we impose subcritical boundary conditions:  $q_{ext} = 8.1 \text{ m}^2/\text{s}$  at  $x = 0 \text{ m}$  and the tidal downstream condition  $\eta_{ext}(t) = 15 + 3 \sin(\omega t) \text{ m}$  at  $x = 1000 \text{ m}$ , with  $\omega = 2\pi/(12 \cdot 3600)$ , that is, a 12-hours tide. As final time we take  $t_f = 3974400 \text{ s}$  (46 days).

Here we start from a flat erodible bottom, which will be affected by the movement of the free surface forced by the tide force. In Figure 6 we see the evolution of the bottom, where we observe see the erosion process and how the upstream condition forces an erosion of the sediment downstream. We see that at final time the thickness of the sediment layer has decreased  $10 \text{ cm}$ .

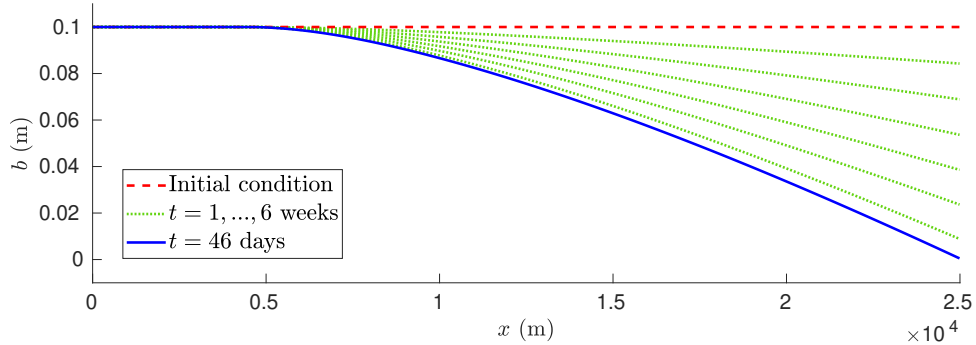


Figure 6: *Test 4.4. Evolution of the sediment till  $t_f = 46$  days (1.5 months), with the  $\Theta$ -method and  $\Delta t = 14 \text{ s}$  ( $C_{cel} \approx 8.1$ ). Dashed red line is the initial condition, dotted green lines correspond to intermediate times and solid blue line is the solution at final time.*

It is remarkable that the value of the discharge is set in order to not having sediment transport

in the whole domain, and just at some times each period of tide, as we can see in Figure 7, where the velocity of the fluid ( $u$ ) and the sediment ( $v_b$  given by (5)) are shown during a period of tide. Bedload takes place just in those nodes verifying  $\theta_{\text{eff}} > \theta_c$ , where we obtain  $v_b \neq 0$ . Depending of the tide, the velocity is growing and decreasing, and just for some times the threshold  $\theta_c$  is exceeded. Actually, we see that a small initial part of the sediment layer (until  $x = 5000$  m approximately) is steady for all times, as it is also observed in Figure 6.

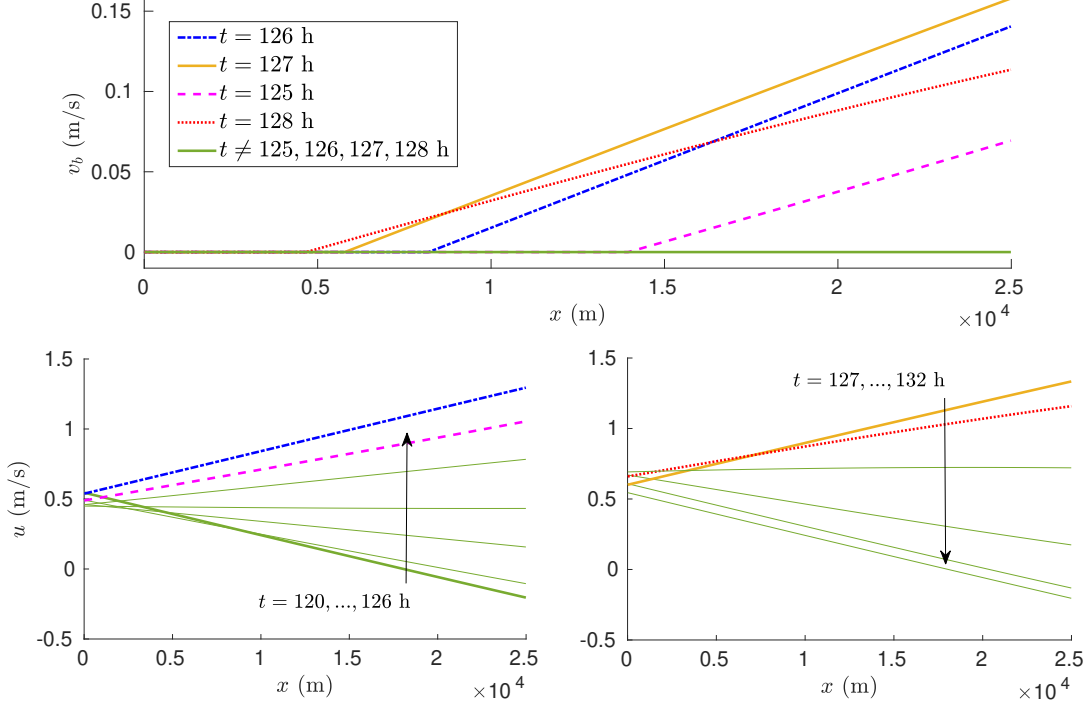


Figure 7: *Test 4.4. Evolution of the sediment velocity  $v_b$  (5) (top figure) and the fluid velocity  $u$  (bottom figures) for a period of tide  $t \in [120, 132]$  h. Green lines correspond to no bedload transport.*

$\Delta t$ (s)	$C_{cel}$	$C_{vel}$	$\text{Err}_\eta [l_2/l_\infty]$ ( $\times 10^{-5}$ )	$\text{Err}_b [l_2/l_\infty]$ ( $\times 10^{-4}$ )	$\text{Err}_u [l_2/l_\infty]$ ( $\times 10^{-4}$ )
5	2.9	0.35	0.3/0.5	0.4/0.5	1.8/1.2
10	5.8	0.70	0.7/0.9	0.9/0.9	3.6/2.5
15	8.7	1.0	1.0/1.4	1.4/1.5	5.4/3.7
20	11.6	1.4	1.3/1.9	1.8/1.8	7.2/4.9
25	14.4	1.7	1.6/2.3	2.2/2.4	8.9/6.1

Table 7: *Test 4.4. Erosion process test: Relative errors with respect to the explicit RK3 with  $C_{cel} = 0.1$ , and Courant numbers reached at final time  $t_f = 46$  days by the semi-implicit method.*

This test involves a long-time simulation and consequently a big computational effort. It must be pointed out that we are using here a coarse mesh to reduce the computational cost, and that

Method	$\Delta t$ (s)	$C_{cel}$	Comp. time (s)	Speed-up
RK3	-	0.9	829.3 (13.8 min)	1
$\Theta$ -method	5	2.9	266.3 (4.4 min)	3.1
$\Theta$ -method	10	5.8	134.4 (2.2 min)	6.2
$\Theta$ -method	15	8.7	89.8 (1.5 min)	9.2
$\Theta$ -method	20	11.6	66.7 (1.1 min)	12.4
$\Theta$ -method	25	14.4	53.7 (0.89 min)	15.4

Table 8: *Test 4.4. Erosion process test: Speed-ups and Courant numbers reached at  $t_f = 46$  days by the semi-implicit method.*

our goal is to show the speed-ups reached for the semi-implicit method with respect to the explicit one. The errors made by the theta method with respect to the explicit RK3 method are not significative for the current configurations, as we see in Table 7. The Courant numbers and the speed-ups reached are shown in Table 8. We see that the semi-implicit method is 15 times faster than the RK3 method without a significant loss of accuracy, which is an important result. As in previous test, we want to comment that we can go further in  $C_{cel}$ , this violating the stability condition based on  $C_{vel}$ .

## 5 Conclusions

An efficient semi-implicit scheme for sediment transport models with gravitational effects under subcritical regimes has been proposed. For the sake of simplicity, here we have chosen the generalization of the Ashida & Michiue’s model, which includes gravitational effects through the definition of  $\tau_{eff}$ . However, this method can be immediately adapted to other models, for both the solid transport discharge and the friction model, by redefining  $Q_b$  in terms of  $\tilde{q}_b$  in (12). Thus, the proposed approach can be adapted to a wide range of families of bedload transport models, as presented in Subsection 2.4. We have also shown that the definition of the effective shear stress,  $\tau_{eff}$ , considered in this paper can be seen as an improved formulation of the one proposed by Fowler *et al.* [19].

An efficient scheme based on the theta method has been proposed following [10], where an iterative Gauss-Seidel algorithm is needed to solve the resulting linear system on  $(\eta, b)$ .

For the considered model an explicit expression for steady states verifying  $Q_b = 0$ . Gravitational terms play a key role on these steady states, since non-physical solutions are obtained if these gravitational terms are neglected. This behavior has been shown in the numerical tests, for both lake at rest and  $u \neq 0$  steady states. In particular, for solutions with  $u \neq 0$  the slope of the steady states is larger than the angle of repose of the sediment.

These gravitational terms also determines the shape of a dune that is swept along by a flow, leading to more realistic (rounded) shapes of the advancing front, where the non-physical shock is corrected. Here we also have shown that a semi-analytic approach, where  $\eta$  and  $q$  are assumed as constant values, gives reasonable results in this case. Finally, an application to erosion processes have been performed, where the time of simulation is very large.

In all the cases, we reduce the computational time of simulations with the proposed semi-implicit method while the accuracy is not notably degraded.



## References

- [1] K. Ashida and M. Michiue. Study on hydraulic resistance and bed-load transport rate in alluvial streams. *Proceedings of the Japan Society of Civil Engineers*, 1972(206):59–69, 1972.
- [2] R. A. Bagnold. *The Flow of Cohesionless Grains in Fluids*. Royal Society of London Philosophical transactions. Series A. Mathematical and physical sciences, no. 964. Royal Society of London, 1956.
- [3] F. Benkhaldoun, M. Seaïd, and S. Sahmim. Mathematical development and verification of a finite volume model for morphodynamic flow applications. *Advances in Applied Mathematics and Mechanics*, 3(4):470–492, aug 2011.
- [4] M. Bilanceri, F. Beux, I. Elmahi, H. Guillard, and M. V. Salvetti. Linearised implicit time-advancing applied to sediment transport simulations. Research Report RR-7492, INRIA, December 2010.
- [5] L. Bonaventura, E. D. Fernández-Nieto, J. Garres-Díaz, and G. Narbona-Reina. Multilayer shallow water models with locally variable number of layers and semi-implicit time discretization. *Journal of Computational Physics*, 364:209–234, 2018.
- [6] M. J. Castro Díaz, E. D. Fernández-Nieto, and A. M. Ferreiro. Sediment transport models in Shallow Water equations and numerical approach by high order finite volume methods. *Computers & Fluids*, 37(3):299–316, March 2008.
- [7] M. J. Castro Díaz, E. D. Fernández-Nieto, A. M. Ferreiro, and C. Parés. Two-dimensional sediment transport models in shallow water equations. A second order finite volume approach on unstructured meshes. *Computer Methods in Applied Mechanics and Engineering*, 198(33-36):2520–2538, jul 2009.
- [8] V. Casulli. Numerical simulation of three-dimensional free surface flow in isopycnal coordinates. *International Journal of Numerical Methods in Fluids*, 25:645 – 658, 1997.
- [9] V. Casulli. A semi-implicit numerical method for the free-surface Navier-Stokes equations. *International Journal for Numerical Methods in Fluids*, 74(8):605–622, nov 2013.
- [10] V. Casulli and E. Cattani. Stability, accuracy and efficiency of a semi-implicit method for three-dimensional shallow water flow. *Computers & Mathematics with Applications*, 27(4):99 – 112, 1994.
- [11] V. Casulli and R. T. Cheng. Semi-implicit finite difference methods for three-dimensional shallow water flow. *International Journal for Numerical Methods in Fluids*, 15(6):629–648, 1992.
- [12] V. Casulli and G. S. Stelling. Numerical simulation of 3d quasi-hydrostatic, free-surface flows. *Journal of Hydraulic Engineering*, 124(7):678–686, 1998.
- [13] V. Casulli and R. A. Walters. An unstructured grid, three-dimensional model based on the shallow water equations. *International Journal of Numerical Methods in Fluids*, 32:331–348, 2000.
- [14] V. Casulli and P. Zanolli. Semi-implicit numerical modelling of non-hydrostatic free-surface flows for environmental problems. *Mathematical and Computer Modelling*, 36:1131–1149, 2002.
- [15] F. Charru. Selection of the ripple length on a granular bed sheared by a liquid flow. *Physics of Fluids*, 18:121508, 2006.
- [16] F. Exner. Über die Wechselwirkung zwischen Wasser und Geschiebe in Flüssen. *Sitzungsber. d. Akad. d. Wiss. pt. IIa. Bd. 134*, 1925.

- [17] R. Fernandez-Luque and R. van Beek. Erosion and transport of bedload sediment. *J. Hydraul. Res.*, 14(2):127–144, 1976.
- [18] E. D. Fernández-Nieto, T. Morales de Luna, G. Narbona-Reina, and J. D. Zabsonré. Formal deduction of the Saint-Venant–Exner model including arbitrarily sloping sediment beds and associated energy. *ESAIM: Mathematical Modelling and Numerical Analysis*, 51(1):115–145, 2017.
- [19] A. C. Fowler, N. Kopteva, and C. Oakley. The formation of river channel. *SIAM J. Appl. Math.*, 67:1016–1040, 2007.
- [20] J. Fredsøe. On the development of dunes in erodible channels. *Journal of Fluid Mechanics*, 64(1):1–16, jun 1974.
- [21] G. Garegnani, G. Rosatti, and L. Bonaventura. Free surface flows over mobile bed: mathematical analysis and numerical modeling of coupled and decoupled approaches. *Communications in Applied and Industrial Mathematics*, 1(3), 2011.
- [22] G. Garegnani, G. Rosatti, and L. Bonaventura. On the range of validity of the Exner-based models for mobile-bed river flow simulations. *Journal of Hydraulic Research*, 51:380–391, 2013.
- [23] J. Garres-Díaz and L. Bonaventura. Flexible and efficient discretizations of multilayer models with variable density. *Applied Mathematics and Computation*, 402:126097, aug 2021.
- [24] A. J. Grass. Sediment transport by waves and currents. 1981.
- [25] P. H. Gunawan, R. Eymard, and S. R. Pudjaprasetya. Staggered scheme for the Exner–Shallow Water equations. *Computational Geosciences*, 19(6):1197–1206, oct 2015.
- [26] L. Hascoët and V. Pascual. TAPENADE 2.1 user’s guide. Technical Report RT-0300, INRIA, 2004.
- [27] C. A. Kennedy and M. H. Carpenter. Additive Runge-Kutta schemes for convection-diffusion-reaction equations. *Applied Numerical Mathematics*, 44:139–181, 2003.
- [28] A. Kovacs and G. Parker. A new vectorial bedload formulation and its application to the time evolution of straight river channels. *Journal of Fluid Mechanics*, 267:153–183, may 1994.
- [29] D. K. Lysne. Movement of sand in tunnels. *Journal of the Hydraulics Division*, 95(6):1835–1846, nov 1969.
- [30] E. Meyer-Peter and R. Müller. Formulas for bed-load transport. *Rep. 2nd Meet. Int. Assoc. Hydraul. Struct. Res., Stockholm*, page 39–64, 1948.
- [31] T. Morales de Luna, M. J. Castro Díaz, and C. Parés Madroñal. A duality method for sediment transport based on a modified Meyer-Peter & Müller model. *Journal of Scientific Computing*, 48(1-3):258–273, dec 2010.
- [32] P. Nielsen. *Coastal Bottom Boundary Layers and Sediment Transport*. WORLD SCIENTIFIC, jul 1992.
- [33] G. Parker, G. Seminara, and L. Solari. Bed load at low shields stress on arbitrarily sloping beds: Alternative entrainment formulation. *Water Resources Research*, 39(7), jul 2003.
- [34] G. Rosatti, L. Bonaventura, A. Deponti, and G. Garegnani. An accurate and efficient semi-implicit method for section-averaged free-surface flow modelling. *International Journal of Numerical Methods in Fluids*, 65:448–473, 2011.
- [35] G. Seminara, L. Solari, and G. Parker. Bed load at low shields stress on arbitrarily sloping beds: Failure of the bagnold hypothesis. *Water Resources Research*, 38(11):31–1–31–16, nov 2002.

- [36] P. A. Tassi, S. Rhebergen, C. A. Vionnet, and O. Bokhove. A discontinuous Galerkin finite element model for river bed evolution under shallow flows. *Computer Methods in Applied Mechanics and Engineering*, 197(33-40):2930–2947, jun 2008.
- [37] L. C. Van Rijn. Sediment Transport, Part I: Bed Load Transport. *Journal of Hydraulic Engineering*, 110(10):1431–1456, 1984.